

Journal of Biomedical Optics

SPIEDigitalLibrary.org/jbo

Empirical relationship between Kubelka–Munk and radiative transfer coefficients for extracting optical parameters of tissues in diffusive and nondiffusive regimes

Arindam Roy
Rajagopal Ramasubramaniam
Harshavardhan A. Gaonkar

Empirical relationship between Kubelka–Munk and radiative transfer coefficients for extracting optical parameters of tissues in diffusive and nondiffusive regimes

Arindam Roy,^a Rajagopal Ramasubramaniam,^a and Harshvardhan A. Gaonkar^b

^aUnilever R&D Bangalore, 64 Main Road, Whitefield, Bangalore, 560066, India

^bIndian Institute of Science Education and Research, Dr. Homi Bhabha Road, Pune, 411008, India

Abstract. Kubelka–Munk (K-M) theory is a phenomenological light transport theory that provides analytical expressions for reflectance and transmittance of diffusive substrates such as tissues. Many authors have derived relations between coefficients of K-M theory and that of the more fundamental radiative transfer equations. These relations are valid only in diffusive light transport regime where scattering dominates over absorption. They also fail near boundaries where incident beams are not diffusive. By measuring total transmittance and total reflectance of tissue phantoms with varying optical parameters, we have obtained empirical relations between K-M coefficients and the radiative transport coefficients for integrating sphere-based spectrophotometers that use uniform, nondiffusive incident beams. Our empirical relations show that the K-M scattering coefficients depend only on reduced scattering coefficient (μ'_s), whereas the K-M absorption coefficient depends on both absorption (μ_a) and reduced scattering (μ'_s) coefficients of radiative transfer theory. We have shown that these empirical relations are valid in both the diffusive and nondiffusive regimes and can predict total reflectance within an error of 10%. They also can be used to solve the inverse problem of obtaining multiple optical parameters such as chromophore concentration and tissue thickness from the measured reflectance spectra with a maximum accuracy of 90% to 95%. © 2012 Society of Photo-Optical Instrumentation Engineers (SPIE). [DOI: 10.1117/1.JBO.17.11.115006]

Keywords: absorption; diffuse reflectance; Kubelka–Munk; radiative transfer; scattering; tissue optics; tissues thickness.

Paper 12470 received Jul. 21, 2012; revised manuscript received Oct. 15, 2012; accepted for publication Oct. 18, 2012; published online Nov. 8, 2012.

1 Introduction

A major challenge in tissue optics is to noninvasively characterize tissue properties for early diagnosis of disease. Optical properties such as scattering (μ_s) and absorption (μ_a) coefficients provide information regarding the morphological and biochemical composition of tissues. Various optical techniques are currently explored to obtain different parameters which represent tissue conditions. One such technique is diffuse reflectance spectroscopy,^{1–4} wherein the spectrum of light reflected from tissue is analyzed to obtain its absorption and scattering properties. Diffuse reflectance needs an accompanying numerical model to decipher the data for obtaining the optical parameters. This can be achieved by solving the radiative transfer equations^{5,6} in tissues. However, due to the complexity of the problem, no analytical solutions exist between the measured reflectance and the optical parameters. Accurate results can be obtained by using Monte Carlo methods,^{7,8} which are inherently very slow. Different authors^{9,10} have developed semi-empirical relations for extracting optical parameters from the reflectance spectra measured using fiber-optic probes with small source-detector separations.

Diffusion approximation of the radiative transfer equation has been used by many authors to obtain optical parameters

such as μ_a and reduced scattering coefficient (μ'_s) from the measured diffused reflectance spectrum.^{11,12} Kubelka–Munk (K-M) theory,¹³ one of the diffusion approximation-based theories, is widely used to obtain optical properties from the measured reflectance spectra. The advantage of this theory is that it provides simple analytical expressions for obtaining the optical parameters from the measured reflectance and transmittance. The reflectance and transmittance of a diffusive media of thickness t is given by

$$R = \frac{(1 - \beta^2)[\exp(\alpha t) - \exp(-\alpha t)]}{(1 + \beta)^2 \exp(\alpha t) - (1 - \beta)^2 \exp(-\alpha t)}$$

$$T = \frac{4\beta}{(1 + \beta)^2 \exp(\alpha t) - (1 - \beta)^2 \exp(-\alpha t)}, \quad (1)$$

where $\alpha = \sqrt{K(K + 2S)}$, $\beta = \sqrt{K/(K + 2S)}$, and K and S are the K-M absorption and scattering coefficients, respectively.

K-M coefficients are only phenomenological approximations, because the theory assumes incident radiation is diffuse and the scattering is isotropic. Similar to other diffusion approximation-based models, K-M theory also assumes higher scattering compared to absorption. Although these conditions are not completely met in many of the real systems, the theory nonetheless provides a simple quantitative way of describing light

Address all correspondence to: Rajagopal Ramasubramaniam, Unilever R&D Bangalore, 64 Main Road, Whitefield, Bangalore, 560066, India. Tel: +91-80-39831041; Fax: +91-80-28453086; E-mail: ram.rajagopal@unilever.com

transport in diffused medium. Many authors^{14–17} have derived relations between the K-M coefficients and the more fundamental radiative transfer coefficients (μ_a , μ_s , and g). Here μ_a is the absorption coefficient, μ_s is the scattering coefficient, and g is the anisotropy factor of the diffusive medium. In the diffusive approximation regime ($\mu_s \gg \mu_a$), the general form of the relations between the K-M coefficients and the radiative transfer coefficients derived by different authors can be written as

$$S = x\mu'_s - y\mu_a \quad K = z\mu_a, \quad (2)$$

where $\mu'_s = \mu_s(1 - g)$ is the reduced scattering coefficient. For an isotropic medium, Klier¹⁴ had shown that $\mu_a = \eta K$ and $\mu_s = \chi S$, and the value of η ranges from 0.5 to 1 and the value of χ ranges from 4/3 to 3.33. van Gemert and Star¹⁵ extended this further to show that the K-M coefficients can be related to the reduced scattering coefficient in an anisotropic medium. For an anisotropic and highly scattering medium, they showed that $K = 2\mu_a$ and $S = (3\mu_s(1 - g) - \mu_a)/4$. However, in most of the measurement geometries, the condition that the incident beam is diffusive is not met. It is either fully collimated or partly collimated and partly diffusive. Various authors have extended this model further to include collimated incident flux and have shown that the K-M theory is also applicable in the case of collimated beam.^{18–20} Thennadil²⁰ has shown that, for a collimated incident beam in the high scattering regime, S depends only on scattering; however, the relation should be modified to include a function dependent on the anisotropy factor, $S = 12\mu'_s/(4.8446 + 0.472g - 0.114g^2)^2$.

Here, we have developed an empirical relationship between the K-M and the radiative transfer coefficients for a collimated incident beam which is valid for both diffusive ($\mu_a \gg \mu'_s$) and nondiffusive ($\mu_a < \mu'_s$) regimes. This was achieved by measuring the total transmittance T (collimated and diffuse) and total reflectance R (diffuse and specular) of tissue phantoms with different set of optical parameters (μ_a and μ'_s) and solving Eq. (1) to obtain the corresponding K-M coefficients K and S . The empirical relations between (K , S) and (μ_a , μ'_s) were obtained, and their applicability for obtaining tissue optical parameters from measured reflectance spectra are discussed in this article.

2 Materials and Methods

2.1 Tissue Phantoms

Liquid tissue phantoms with different optical parameters were prepared in a 0.75-mm-thick glass cuvet by dispersing known concentrations of polystyrene microspheres and one of the two brown colored dyes in milliQ water. The Premium Dark Chocolate dye was procured from Devarsons Industries, India, and the Chocolate Brown TAS dye was procured from Roha Dyechem, India. Polystyrene microspheres of 0.5- and 1- μm diameter were procured from Duke Scientific, USA. Absorption coefficients of the dyes and the scattering coefficient (μ_s) of the polystyrene spheres were measured using a Perkin Elmer Lambda900 UV-Vis spectrophotometer. The wavelength-dependent absorption coefficients of the two dyes for 10 ppm concentration are shown in Fig. 1. The anisotropy factor g was calculated using a web-based Mie scattering calculator developed by Philip Laven.²¹ The reduced scattering coefficients were calculated using the relation $\mu'_s = \mu_s(1 - g)$.

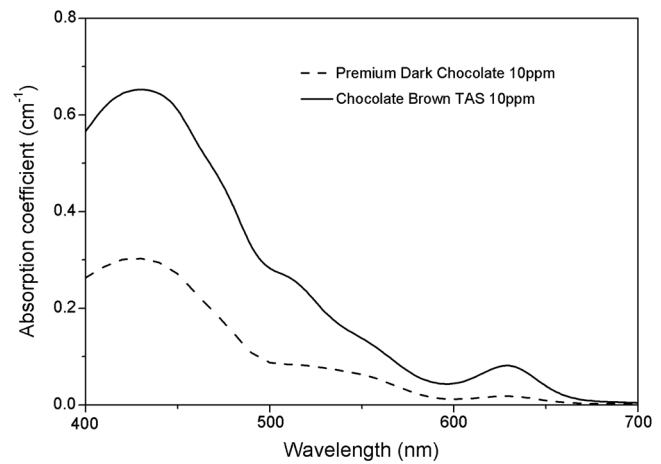


Fig. 1 Absorption spectra of the colored dyes used in the tissue phantoms.

2.2 Spectral Measurements

Total transmittance (collimated and diffuse) and total reflectance (specular and diffuse), at 488 nm, of the tissue phantoms were measured using an Ar-ion laser (Lexel, USA), a 90-mm-diameter integrating sphere (Labsphere, USA), and a spectrometer (ILT 900 from International Light, USA). The configurations used in these measurements are shown in Fig. 2(a) and 2(b). Reflectance was measured relative to a Spectralon® reflectance standard with a reflectance value of 99% in the 400- to 650-nm range. For reflectance measurement, the sample was held at 8 deg with respect to the direction of normal incidence, as shown in Fig. 2(a), to include the specular component of the reflected beam. The specular and the diffuse reflected light was collected by the integrating sphere and measured using the spectrometer. Reflectance from a water-filled reference cuvet was subtracted from the measured reflectance to obtain reflectance from the tissue phantom alone. During total transmittance measurement, the transmitted light was collected by an integrating sphere and measured using a spectrometer as shown in Fig. 2(b). A water-filled cuvet was used as reference during transmittance measurements to account for reflectance losses from the cuvet walls.

For the validation study, the wavelength-dependent reflectance spectra were measured using a handheld spectrophotometer (CM-2600d, Minolta, Japan). The configuration of the spectrophotometer is shown in Fig. 2(c). It is equipped with two pulsed Xenon lamps and a 52-mm-diameter integrating sphere. The sample was illuminated through an 8-mm-diameter aperture. The integrating sphere and the small aperture ensure that a broad collimated beam is incident on the sample. The reflected light is collected through the same aperture in the 8-deg viewing angle and is analyzed using a diffraction grating and a photodiode array. The reflectance was measured in the wavelength range of 400 to 650 nm with a spectral resolution of 10 nm.

3 Results

3.1 Empirical Relations between K-M and Radiative Transfer Coefficients

The method used to obtain the empirical relations between the radiative transfer and K-M coefficients is schematically shown in Fig. 3. First, the total reflectance (R) and total transmittance

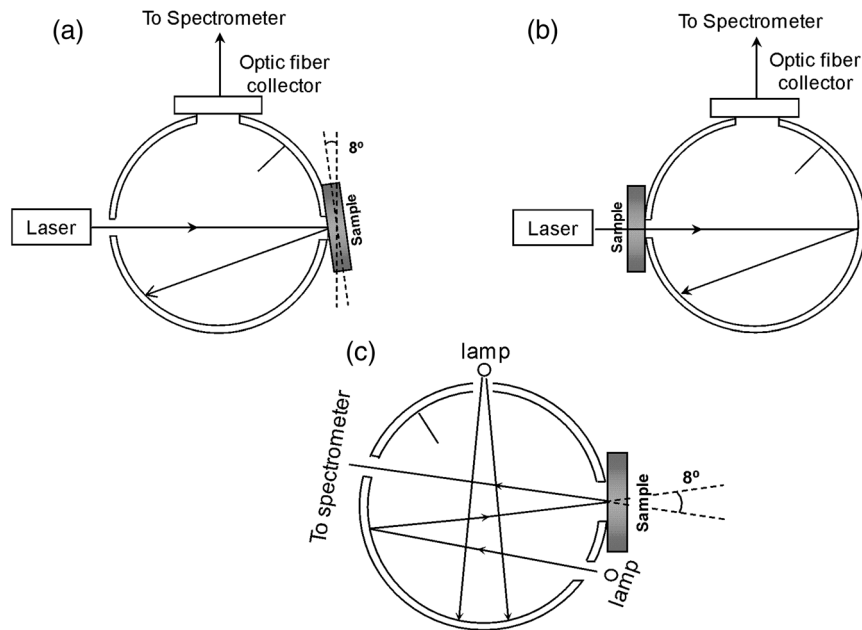


Fig. 2 Measurement configuration used to measure total reflectance (a) and total transmittance (b). (c) Measurement configuration of the commercial spectrophotometer used in validation measurements.

(T) values of a diffusive layer were measured for various sets of μ_a and μ'_s . For a given set of R and T values, there is a unique set of K and S values that can be obtained by solving the coupled relations shown in Eq. (1). Finally, empirical relationships are obtained between the calculated sets of K and S values and the sets of radiative transfer coefficients (μ_a and μ'_s) used in the tissue phantom.

For R and T measurements, tissue phantoms with six different μ'_s values—0, 0.22, 0.41, 0.54, 0.81, and 1.63 mm^{-1} —were obtained by varying the concentration of the 0.5- μm -diameter microspheres. For a constant μ'_s , μ_a was varied from 0 to 0.25 mm^{-1} by varying the concentration of the Premium Dark Chocolate dye shown in Fig. 1. The measured T and R values for various values of μ_a and μ'_s at 488 nm are shown in Fig. 4. For increasing μ_a , both R and T decrease. With increasing μ'_s , T decreases while R increases. The measured R and T values are functions of K and S as shown in Eq. (1), which in turn depend on μ_a and μ'_s .

Earlier authors^{18–20} have shown that the K-M theory is also applicable to collimated incident beam in the regime where $\mu'_s \gg \mu_a$. In the current measurement geometry, the incident

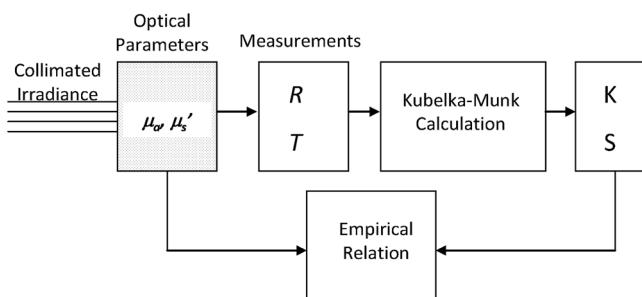


Fig. 3 Schematic diagram of the method used to obtain empirical relations between radiative transport coefficients and the Kubelka–Munk (K-M) coefficients. From the measured total reflectance (R) and transmittance (T), the K-M coefficients were calculated and related to the tissue phantom’s radiative transport coefficients (μ_a and μ'_s).

beam is collimated. However, not all the tissue phantoms fall in the regime $\mu'_s \gg \mu_a$. Assuming that K-M theory is applicable for all ranges of μ_a and μ'_s , including $\mu_a \geq \mu'_s$, the values of K and S were calculated by solving the coupled equations in Eq. (1) for various values of R and T shown in Fig. 4. The

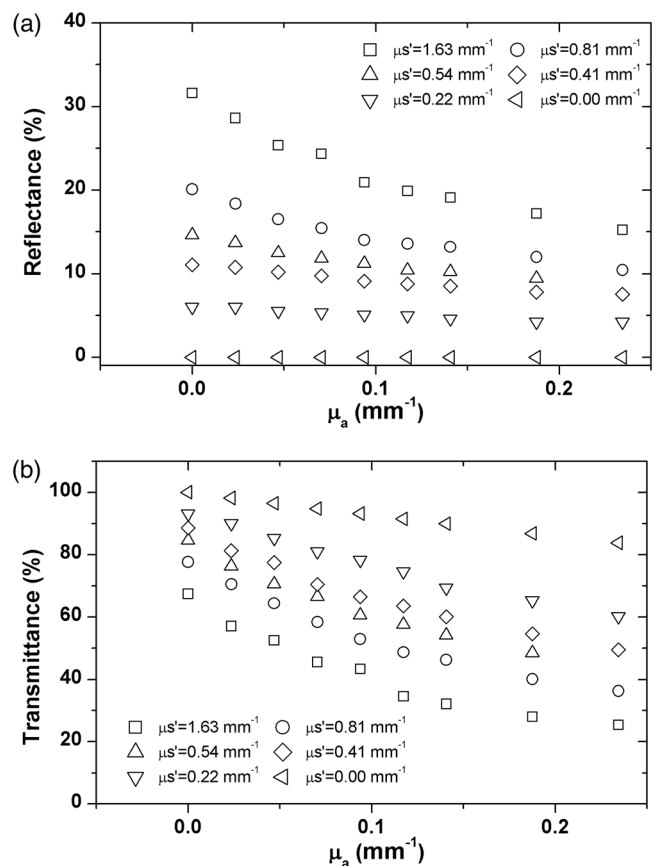


Fig. 4 Measured values of total reflectance (a) and total transmittance (b) at 488 nm of tissue phantoms for various values of μ_a and μ'_s .

calculated S and K values are plotted as a function of μ_a for constant values of μ'_s and are shown in Fig. 5(a) and 5(b), respectively.

From Fig. 5(a), it is clear that S depends strongly on μ'_s and not on μ_a even in the diffusive regime $\mu'_s \gg \mu_a$. This is different from earlier reports which showed that the S depends on μ_a and μ'_s as shown in Eq. (2). Our measurement agrees with derivations of Gate¹⁷ and Thennadi²⁰ where y was zero. By fitting the experimental values to Eq. (2), we find the value of x to be 0.408. Thus

$$S = 0.408\mu'_s. \quad (3)$$

Figure 5(b) shows the dependence of K as a function of μ_a and μ'_s . Unlike S , K depends on both μ_a and μ'_s . K-M absorption coefficient K increases as μ_a increases. In the absence of scattering, K is equivalent to the absorption coefficient μ_a . Increasing μ'_s at a given μ_a further increases K . In the presence of scattering, K has an additional term which we can attribute to the absorption due to scattered photons. The absorption of the scattered photon depends not only on the absorption coefficient of the medium but also on the mean average distance traveled by the scattered photon, which is proportional to its scattering coefficient.¹⁰ A photon in a highly scattering medium will travel larger distances compared to a photon in a low-scattering medium. Hence the effective absorption of the

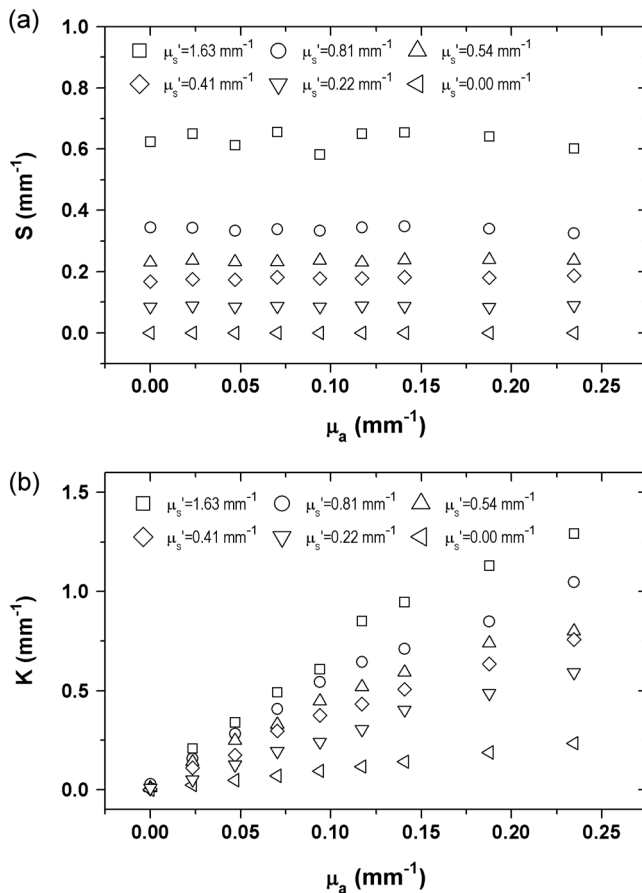


Fig. 5 K-M scattering coefficient S (a) and K-M absorption coefficient K (b) for tissue phantoms with various values of μ_a and μ'_s . K and S were obtained from the measured total reflectance (R) and total transmittance values (T) by solving the K-M equations.

scattered photon will depend on both the absorption coefficient and the scattering coefficient. We find that K follows the following empirical relation:

$$K = \mu_a + a(\mu_a\mu'_s)^b, \quad (4)$$

where μ_a and μ'_s are expressed in units of mm^{-1} . By fitting our data to the above empirical relation, we find the parameter values as $a = 2.43$ and $b = 0.72$. Figure 6 shows predicted values of S and K using the empirical relations in Eqs. (3) and (4) against values of S and K calculated from measured R and T values using Eq. (1). We see an excellent fit, with R^2 values of 0.97, implying that our empirical relation is applicable to a wide range of μ_a and μ'_s .

3.2 Validation of Empirical Relations Using Tissue Phantoms

To validate the applicability of the empirical relations in Eqs. (3) and (4), tissue phantoms were prepared using 1- μm polystyrene spheres and five different concentrations (0, 10, 20, 30, and 40 ppm) of the Chocolate Brown TAS dye whose extinction coefficient is shown in Fig. 1. Total reflectance of the tissue phantoms was measured in the wavelength range of 400 to 650 nm using a commercial spectrophotometer as shown in Fig. 2(c). In this range, there is large variation of absorption as a function of wavelength. In certain regions $\mu_a < \mu'_s$; in other regions $\mu_a \geq \mu'_s$. Because μ'_s and μ_a of the tissue phantoms are known for all the wavelengths, K and S values can be calculated using Eqs. (3) and (4), and the reflectance for the entire wavelength range can then be predicted using Eq. (1).

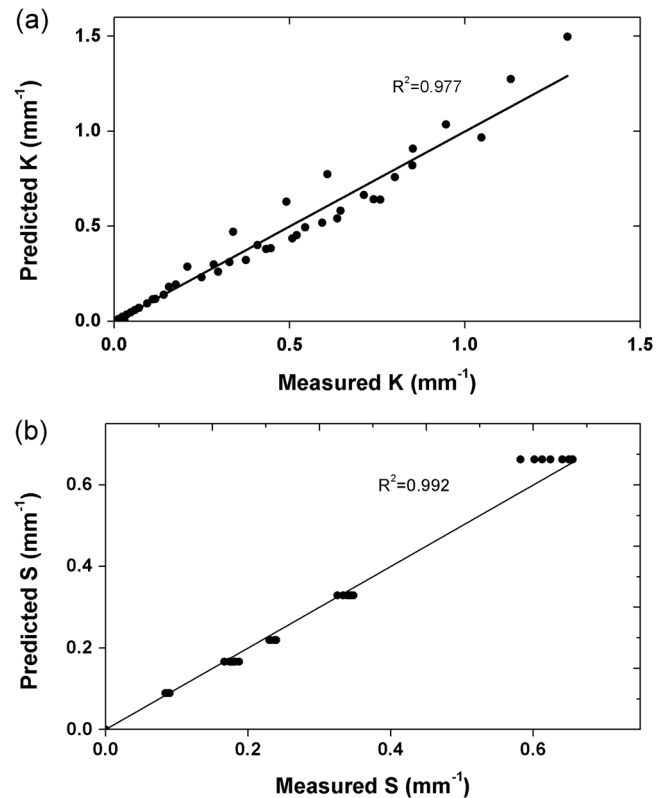


Fig. 6 Predicted values of S and K using the empirical relations in Eqs. (3) and (4) as a function of S and K values calculated from measured R and T using Eq. (1).

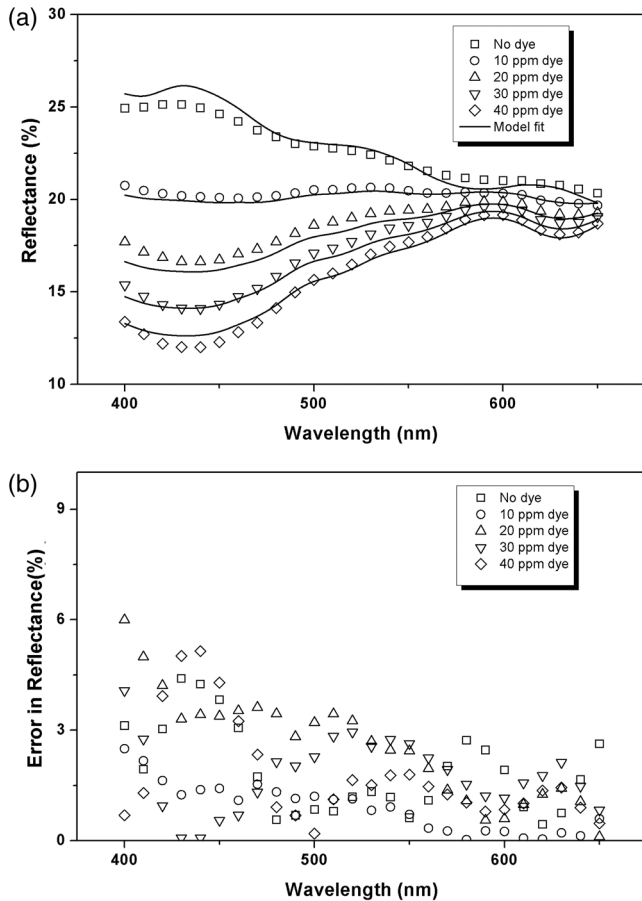


Fig. 7 (a) Measured reflectance spectra and predicted reflectance spectra for tissue phantoms with different concentrations of the Chocolate Brown TAS dye. (b) Error in prediction.

In Fig. 7(a), the measured reflectance spectra (dots) of tissue phantoms with various dye concentrations are shown along with the reflectance spectra predicted (solid lines) using Eqs. (3) and (4). Good agreement was obtained between the predicted and measured reflectance spectra. The maximum errors in the predictions are shown in Fig. 7(b). The maximum error in prediction was about 6%, implying that the empirical relation between the optical parameters and K-M coefficient is valid over a wide range of optical parameters.

3.3 Extracting Optical Parameters from Measured Reflectance

Because the empirical relations in Eqs. (3) and (4) are valid over wide range of optical parameters and wavelengths, it is possible to solve the inverse problem of extracting various optical parameters from the measured reflectance spectra. For example, parameters such as concentration of the chromophores and thickness of the scattering layer can be extracted simultaneously from the measured reflectance if the scattering parameters are known. This is feasible, since at different wavelengths, relations in Eqs. (3) and (4) are valid and independent of each other. One needs to solve for two unknown parameters using more than two equations. To verify the feasibility of simultaneously extracting dye concentration and layer thickness from the measured reflectance, tissue phantoms of two different thicknesses (450 and 750 μm) were prepared using 1000-nm polystyrene spheres

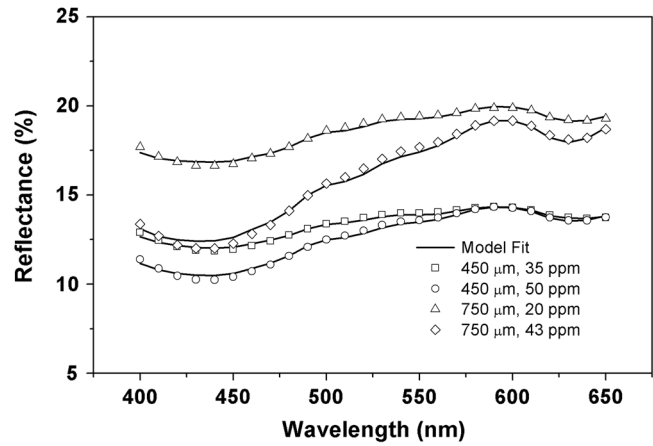


Fig. 8 Solving for optical parameters from the measured reflectance spectra of tissue phantoms. The best fits were obtained by varying two fitting parameters, namely dye concentration and layer thickness. The symbols show measured reflectance, and solid lines show the best fit from the model. The actual parameter values and the predicted values are shown in Table 1.

and different concentrations of the Chocolate Brown TAS dye shown in Fig. 1. The reflectance of the tissue phantoms in the range of 400 to 650 nm was measured, and best fits to the reflectance curves were obtained using Eqs. (1), (3), and (4) by freely varying the two fitting parameters, namely the concentration of the dye and thickness of the phantom layer. The best fit obtained is shown in Fig. 8, and the parameters used to obtain the best fit are shown in Table 1 along with the actual parameters. The extracted concentration values were within an error of 2% to 10% whereas the extracted thickness values were within 2% error.

4 Discussion

In most biological tissues, diffusion approximation is valid only in the wavelength region between 600 and 900 nm where scattering is larger than the absorption. Sometimes, even in the highly scattering regime, collimated incident beams do not become diffusive if the tissues studied are very thin. For example, the epidermis of skin is only about 50 to 100 μm thick, where absorption is more than the scattering in the 400-

Table 1 Actual and extracted values of dye concentrations and phantom thicknesses along with error in prediction.

Concentration			Thickness		
Actual (ppm)	Extracted (ppm)	Error (%)	Actual (μm)	Extracted (μm)	Error (%)
35	32	8.6	450	444	1.3
50	49	2.0	450	455	1.1
20	18.1	9.5	750	752	0.3
43	45	4.7	750	763	1.7

The dye concentration and phantom thickness were used as fitting parameters in the model and simultaneously varied to obtain the best fit to the reflectance curves shown in Fig. 8.

600-nm region and the transport is not diffusive.²² Also, in most of the measurement geometries, light is not diffusive, especially near the tissue boundaries. Hence, most of the diffusion theory-based models relating K-M coefficients to the radiative transfer coefficients have limited practical applicability. In this paper, a simple and practical empirical relation is developed between K-M and radiative transfer coefficients for a collimated incident beam (either narrow or broad), which is typical of most of the measurement geometries, for example, integrating sphere-based reflectance measurements. The relations developed are also shown to be applicable in the nondiffusive regimes where absorption is larger than scattering.

The empirical relation in this model was derived by measuring the total reflectance and total transmittance of the tissue phantoms. One of the key challenges in measuring total reflectance using integrating sphere geometry is the collection of all scattered light with minimal loss. An incident beam diverges within the sample due to scattering, and the reflected beam size is always larger than the incident beam. In the case of thin or low-scattering samples, the beam divergence will be minimal and hence the error in reflectance measurement will be small. For thick and highly scattering samples, the divergence of the beam will be higher. The error in reflectance measurement can increase, thereby decreasing the accuracy of this method. This error can be reduced by the use of integrating spheres with a larger aperture size. In the current study, we find that, in the typical tissue scattering regime ($\mu'_s = 0.5\text{--}2\text{ mm}^{-1}$), the empirical relations seem to work well with less than 10% error in solving the inverse problem.

Most of the existing empirical models for studying tissue reflectance are applicable only to homogeneous tissues and cannot be extended to inhomogeneous or layered tissues. Many authors have developed multi-layer models to describe reflection from inhomogeneous tissues. Similarly, since the K-M theory provides analytical expression of both transmittance and reflectance of the diffusive layers, it can be extended to describe layered tissues also. If R_1, R_2, \dots, R_n and T_1, T_2, \dots, T_n are the reflectance and transmittance of the different layers that can be calculated using Eq. (1) and the empirical relations shown in Eqs. (3) and (4), then the total reflectance and transmittance of the layers can be calculated in the following way. If I_n is the light flux traveling in the forward direction and J_n is the light traveling in the reverse direction from the n th layer, respectively, then we can write

$$\begin{aligned} I_1 &= I_0 T_1 + J_1 R_1 \text{ and } J_0 = J_1 T_1 + I_0 R_1 \\ I_2 &= I_1 T_2 + J_2 R_2 \text{ and } J_1 = J_2 T_2 + I_1 R_2 \\ &\vdots \\ I_n &= I_{n-1} T_n + J_n R_n \text{ and } J_{n-1} = J_n T_n + I_{n-1} R_n \end{aligned} \quad (5)$$

The total reflectance $R = J_0$ and total transmittance $T = I_n$. With $I_0 = 1$ and $J_n = 0$ as boundary conditions, these equations can be solved self-consistently to obtain the values of $R = J_0$. For example, for a two-layer tissue, solving Eq. (5) self-consistently results in the following relation:

$$R = R_1 + \frac{T_1^2}{1 - R_1 R_2} \quad \text{and} \quad T = \frac{T_1 T_2}{1 - R_1 R_2}. \quad (6)$$

Similarly, for a tissue with inhomogeneous distribution of chromophores, a multilayer model can be built by discretizing

the layers with a distribution of absorption and scattering coefficients. However, like any other multilayer model, the current model also will have multiple parameters describing the layers, and hence one needs to solve the inverse problem of obtaining these parameters from the measured reflectance.

5 Conclusions

In summary, by measuring total transmittance and total reflectance of tissue phantoms with varying optical parameters, we have obtained empirical relations between K-M coefficients and the radiative transport coefficients for integrating sphere-based spectrophotometers that use uniform, nondiffusive incident beams. We have shown that the K-M scattering coefficient depends only on reduced scattering coefficient, while the K-M absorption coefficient depends on both the absorption and reduced scattering coefficients of the radiative transfer theory. We have also shown that these empirical relations are valid in both the diffusive and nondiffusive regimes. Using these relations, we could predict reflectance spectra of tissues within an error of 6%. The empirical relations were used to predict the chromophore concentration and the tissue thickness simultaneously by solving the inverse problem from the measured reflectance. The error in the prediction of chromophore concentration and tissue thickness was less than 10%.

References

1. B. W. Murphy et al., "Toward the discrimination of early melanoma from common and dysplastic nevus using fiber optic diffuse reflectance spectroscopy," *J. Biomed. Opt.* **10**(6), 064020 (2005).
2. F. Koenig et al., "Spectroscopic measurement of diffuse reflectance for enhanced detection of bladder carcinoma," *Urology* **51**(2), 342–345 (1998).
3. I. J. Bigio et al., "Diagnosis of breast cancer using elastic-scattering spectroscopy: preliminary clinical results," *J. Biomed. Opt.* **5**(2), 221–228 (2000).
4. J. R. Mourant et al., "Spectroscopic diagnosis of bladder cancer with elastic light scattering," *Lasers Surg. Med.* **17**(4), 350–357 (1995).
5. A. Ishimaru, *Wave Propagation and Scattering in Random Media*, Vol. 1, Academic Press, New York (1978).
6. K. M. Case and P. F. Zweifel, *Linear Transport Theory* Addison-Wesley, Reading, PA (1967).
7. B. C. Wilson and G. Adam, "A Monte Carlo model for the absorption and flux distributions of light in tissue," *Med. Phys.* **10**(6), 824–830 (1983).
8. S. A. Prahl et al., "A Monte Carlo model of light propagation in tissue," *Proc. SPIE* **IS 5**, 102–111 (1989).
9. G. Mantis and G. Zonios, "Simple two-layer reflectance model for biological tissue applications," *Appl. Opt.* **48**(18), 3490–3496 (2009).
10. R. Reif, O. A' Amar, and I. J. Bigio, "Analytical model of light reflectance for extraction of the optical properties in small volumes of turbid media," *Appl. Opt.* **46**(29), 7317–7318 (2007).
11. T. J. Farrell, M. S. Patterson, and B. C. Wilson, "A diffusion theory model of spatially resolved, steady-state diffuse reflectance for the non-invasive determination of tissue optical properties *in vivo*," *Med. Phys.* **19**(4), 879–888 (1992).
12. A. Kienle and M. S. Patterson, "Improved solutions of the steady-state and the time resolved diffusion equations for reflectance from a semi-infinite turbid medium," *J. Opt. Soc. Am. A* **14**(1), 246–254 (1997).
13. P. Kubelka and F. Munk, "Ein Beitrag zur Optik der Farbanstriche," *Zeits. f. tech. Physik* **12**, 593–601 (1931).
14. K. Klier, "Absorption and scattering in plane parallel turbid media," *J. Opt. Soc. Am.* **62**(7), 882–885 (1972).
15. M. J. C. van Gemert and W. M. Star, "Relations between the Kubelka–Munk and transport equation models for anisotropic scattering," *Lasers Life Sci.* **1**, 287–298 (1987).

16. B. J. Brinkworth, "Interpretation of the Kubelka–Munk coefficients in reflection theory," *Appl. Opt.* **11**(6), 1434–1435 (1972).
17. L. F. Gate, "Comparison of the photon diffusion model and Kubelka–Munk equation with the exact solution of the radiative transport equation," *Appl. Opt.* **13**(2), 236–238 (1974).
18. J. T. Atkins, "Absorption and scattering of light in turbid media," Ph. D. Dissertation, (University of Delaware, 1965).
19. J. Reichman, "Determination of absorption and scattering coefficients for non-homogeneous media. 1: theory," *Appl. Opt.* **12**(8), 1811–1815 (1973).
20. S. N. Thennadil, "Relationship between the Kubelka–Munk scattering and radiative transfer coefficients," *J. Opt. Soc. Amer. A.* **25**(7), 1480–1485 (2008).
21. Philip Laven, "A computer program for scattering of light from a sphere using Mie theory & the Debye series," <http://www.philiplaven.com/mieplot.htm> (October 24, 2012).
22. T. Igarashi, K. Nishino, and S. Nayar, "The appearance of human skin," Tech. Rep. CUCS-024-05, Department of Computer Science, Columbia University (2005).